Chemical Science

EDGE ARTICLE

View Article Online
View Journal | View Issue

Evaluating atomic components in fluorene wires†

Cite this: *Chem. Sci.*, 2014, **5**, 1561

Received 7th January 2014
Accepted 30th January 2014

DOI: 10.1039/c4sc00064a

www.rsc.org/chemicalscience

R. S. Klausen,‡[a] J. R. Widawsky,[b] T. A. Su,[a] H. Li,[b] Q. Chen,[a] M. L. Steigerwald,[a] L. Venkataraman[b] and C. Nuckolls[a]

Molecular electronics demands complex functional molecules with multiple pathways connecting electrode leads. We report the synthesis and study of a set of molecules based on a fluorene-like design in which atomic connectors are used to introduce two pathways for conductance. This manuscript details the structural demands and underlying rationale for developing high conductance in these complex molecular circuit components.

Introduction

This report evaluates the difference in well-defined atomic connections within a molecular circuit as they are varied from silicon to oxygen to nitrogen. The test series is a set of substituted 3,6-dithiomethylfluorenes in which we replace the methylene at the 9-position with $SiPh_2$, O, and NPh (Fig. 1). We show that neither the dibenzosilole (**1**) nor the dibenzofuran (**2**) conduct, yet the carbazole (**3**) does. The lone pair on N is a viable electrical conduit while neither the lone pair on O nor the Si–C bonds are. The key to uncovering this unique trend is the rigid locking of the atomic elements into the organic framework. In these constrained geometries, we find that the stereoelectronics of the atomic connection defines the conductance.

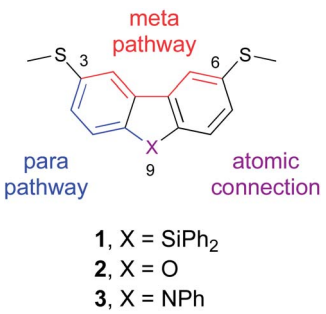

Fig. 1 Molecular structure of compounds **1**–**3**.

The 9-substituted, 3,6-dithiomethylfluorene family is a platform for determining the relative electrical conductivities of X. It has been shown, both by ourselves and others, that a phenyl ring can either be a very conductive element or a very resistive element depending on the substitution pattern around the ring: *para* disubstitution of two conductive linking groups generally yielding the former, and *meta* disubstitution yielding the latter.[1–6] The fluorene backbone is planar and the *meta* pathway (shown in red) is electrically non-conductive.[7] Therefore, any conductance through a 9-substituted fluorene occurs through the *para* pathway (shown in blue) and consequently depends on the ability of X to electrically couple to the biphenyl framework.

Results and discussion

We prepare dibenzosilole **1** by the sequence shown in Fig. 2. Full details and characterization can be found in the ESI.† First, we utilize a Suzuki–Miyaura coupling[8,9] followed by a dibromination reaction to furnish **4**. Next, we subject **4** to a double lithium halogen exchange[10,11] followed by reaction with dichlorodiphenylsilane to yield **1**. Compounds **2** and **3** were synthesized from the commercially available dibromides *via* double lithiation and reaction with dimethyl disulfide.

Throughout this study, we measure single molecule conductance using a scanning tunneling microscope break junction (STM-BJ) technique in which we repeatedly form and break gold point contacts in a solution of the target molecule at room temperature and low voltage bias.[12,13] After the Au–Au

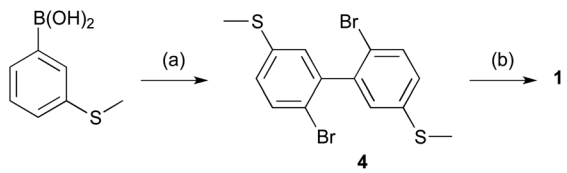

Fig. 2 [a]Key: (a) (i) $Pd(PPh_3)_4$, Na_2CO_3, 3-bromothioanisole, 80 °C, 98% yield. (ii) Br_2, AcOH, 76% yield. (b) *n*BuLi, −78 °C then Ph_2SiCl_2, 66% yield.

[a]Department of Chemistry, Columbia University, New York, NY, 10027, USA

[b]Department of Physics and Applied Mathematics, Columbia University, New York, NY 10027, USA

† Electronic supplementary information (ESI) available: Experimental and synthetic procedures, characterization data, details of computational methods. See DOI: 10.1039/c4sc00064a

‡ Present address: Department of Chemistry, The Johns Hopkins University, Baltimore, MD, 21218, USA.

point contact is broken, aurophilic methyl sulfide groups on the molecule bind to undercoordinated gold atoms to form Au–molecule–Au junctions.[14] Conductance (current/voltage) is measured across the gap as a function of tip–substrate separation, and the resulting traces reveal molecule-dependent plateaus denoting junction formation with conductance values below $G_0(2e^2/h)$, the quantum of conductance describing a single Au–Au contact. Junctions are formed and broken thousands of times and the corresponding traces are used to generate statistical histograms without data selection.[15] One-dimensional histograms show the frequency of conductance values measured averaged over all traces. Two-dimensional histograms reveal the junction conductance evolution as a function of elongation.[16] These are created by aligning the displacement axis of all traces at zero displacement prior to generating the histogram.

Fig. 3a compares the 1D conductance histograms of **1–3**. We found that the conductance histograms of **1** (red) and **2** (blue) are largely featureless and similar to clean gold (yellow).[17] A small feature at $10^{-3}G_0$ in the blue trace corresponding to compound **2** does not correspond to a molecular junction (junction length <0.1 nm, see Fig. S1†). In contrast, the conductance histogram of the carbazole **3** (black) shows a well-defined peak with a value of $9 \times 10^{-4}G_0$, and the two-dimensional histogram created from the same set of traces shows a clear feature starting at zero displacement and extending to 0.4 nm. This feature is similar to those observed for measurements of other compounds of similar length.[18]

The lack of conductance in silane **1** is particularly surprising in light of our earlier study showing that organosilanes conduct as well as conjugated oligoenes.[18] To study the origin of the insulating behavior in **1** and **2**, we synthesized and tested 3,3′-(methylthio)biphenyl **5**, the "unlocked" *meta* pathway contained in **1**. Biphenyl **5** does not show a clear conductance peak either (green). We also note that fluorene-like molecules in which the anchor groups (both H_2N– and AcS–) are disposed *para* to the biphenyl bridge have been synthesized and single molecule conductance measurements show that such molecules conduct comparably to biphenyl itself.[19,20] We have synthesized the *meta*-linked structural isomer and show that it does not conduct within the measurable range (see ESI† for details). Such control experiments further highlight the unique conductance behaviour of the *meta*-linked carbazole.

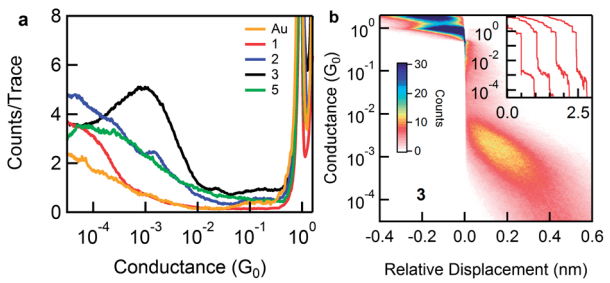

Fig. 3 (a) Logarithmically-binned conductance histograms for compounds **1–3**, **5**, and clean gold (shown as control). These histograms are each constructed with 100 bins per decade from >10 000 traces (5000 for Au) and without any data selection. (b) Two-dimensional histogram of carbazole **3** constructed from the same data used to create the 1D histogram shown in (a). The $1G_0$ peak is visible at negative displacements and the clear molecular signature is visible at positive displacement. The inset shows sample conductance traces which are offset laterally for clarity.

We studied the electronic structure of **1–3** and **5** using density functional theory based calculations to ascertain why **3** alone conducts.[21] In Table 1, we show the two highest-energy occupied molecular orbitals (HOMO and HOMO−1) for **1–3**. It has been shown previously that for junctions formed using the same type of linkers, molecular conductance increases as the difference in energy between the Au Fermi level and the closest molecular orbital decreases.[22–26] We find that the HOMO levels of **1** and **2** are very similar (−5.64 eV and −5.66 eV, respectively), but the HOMO of **3** is much higher (−5.08 eV).[21] In each pair of orbitals for **1–3** in Table 1, the amplitude on each sulfur atom is pronounced and equal in magnitude; thus, each pair of occupied orbitals describes the S p–π lone pairs on opposite sides of the molecule.[27] The splitting in energy between the HOMO and HOMO−1 indicates the extent to which the two distal sulfurs are electrically connected: a small splitting indicates two independent lone pairs and weak delocalization.[28] Likewise, a large splitting indicates the two lone pairs are strongly interacting. In addition to the higher HOMO energy as noted above, the splitting is significantly larger in **3**, indicating a more strongly coupled set of S lone pairs in **3** than in **1** and **2**.[29] All of these data are consistent with our experimental discovery that **3** is much more conductive than **1** and **2**.

Table 1 Representations and energies of the calculated highest occupied molecular orbital (HOMO) and HOMO−1 energies of **1–3** and **5** at the B3LYP/cc-pVTZ level of DFT

Molecule	HOMO (eV)	HOMO−1 (eV)	Splitting (eV)
1	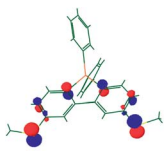 -5.64	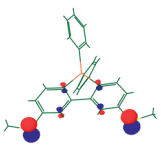 -5.92	0.28
2	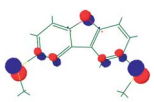 -5.63	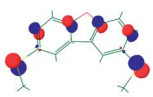 -5.82	0.19
3	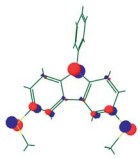 -5.08	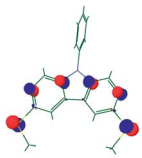 -5.58	0.50
5	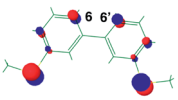 -5.77	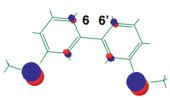 -5.98	0.22

The stereoelectronic properties of the combination of the N-centered lone pair and the 3,3′-(methylthio)biphenyl cause both of these effects. While the HOMO and HOMO−1 of 3,3′-(methylthio)biphenyl **5** are primarily sulfur-centered, there is significant electron density on the carbons *para* to the sulfur substituents (carbons 6 and 6′). When an atom X bridges the 6 and 6′ carbons to form the fluorene framework, the extent to which the orbitals in X interact with the orbitals of the aromatic group determines the strength of the coupling between the sulfur lone pairs in the resulting molecule.[30] The p–π lone pair on the nitrogen in the carbazole interacts more strongly with the two sulfur lone pair orbitals *via* the intervening aromatic rings than either the oxygen or silane. This is a function of both geometry and energetics. The $SiPh_2$ has an sp^3 geometry that is not optimal for overlap with the π orbitals of the rigid, planar biphenyl rings. Both O and N can attain an sp^2-geometry which places a filled p-orbital in the correct geometry; however the orbital containing the O lone pair is too small and its energy too low for effective overlap. The N lone pair combines both the correct geometry and ideal energetics. These conclusions are supported both by the orbital surfaces and observed orbital energy splittings. The fact that the energies of the sulfur lone pair orbitals increase on going from biphenyl **5** to carbazole **3** indicates that the interaction between these doubly-occupied orbitals is repulsive. The presence of the lone p–π pair on N in **3** creates strong coupling between the two sulfur centers. Since one sulfur binds to each of the electrodes in the STM-BJ measurement, the nitrogen lone pair also insures strong coupling between the two electrodes and a conductive pathway is established.

Conclusions

Herein, we rationalize an exception to the low-conductance observed in *meta*-linked molecules. Our results highlight the importance of through-bond coupling in molecular conductance. Moreover, this study suggests that variable coupling may serve as a design principle in switchable single molecule circuits and sensors.[31]

Acknowledgements

STM-BJ experiments were supported as part of the Center for Re-Defining Photovoltaic Efficiency Through Molecular-Scale Control, an Energy Frontier Research Center funded by the U.S. Department of Energy (DOE), Office of Science, Office of Basic Energy Science under award number DE-SC0001085. H. L. is supported by the Semiconductor Research Corporation and New York CAIST program. T. A. S. is supported by a National Science Foundation pre-doctoral fellowship.

Notes and references

1 G. C. Solomon, D. Q. Andrews, T. Hansen, R. H. Goldsmith, M. R. Wasielewski, R. P. Van Duyne and M. A. Ratner, *J. Chem. Phys.*, 2008, **129**, 054701.
2 G. C. Solomon, D. Q. Andrews, R. H. Goldsmith, T. Hansen, M. R. Wasielewski, R. P. Van Duyne and M. A. Ratner, *J. Am. Chem. Soc.*, 2008, **130**, 17301.
3 M. Mayor, H. B. Weber, J. Reichert, M. Elbing, C. von Hänisch, D. Beckmann and M. Fischer, *Angew. Chem., Int. Ed.*, 2003, **42**, 5834.
4 C. M. Guedon, H. Valkenier, T. Markussen, K. S. Thygesen, J. C. Hummelen and S. J. van der Molen, *Nat. Nanotechnol.*, 2012, **7**, 305.
5 J. S. Meisner, S. Ahn, S. V. Aradhya, M. Krikorian, R. Parameswaran, M. L. Steigerwald, L. Venkataraman and C. Nuckolls, *J. Am. Chem. Soc.*, 2012, **134**, 20440.
6 S. V. Aradhya, J. S. Meisner, M. Krikorian, S. Ahn, R. Parameswaran, M. L. Steigerwald, C. Nuckolls and L. Venkataraman, *Nano Lett.*, 2012, **12**, 1643.
7 A. Mishchenko, D. Vonlanthen, V. Meded, M. Burkle, C. Li, I. V. Pobelov, A. Bagrets, J. K. Viljas, F. Pauly, F. Evers, M. Mayor and T. Wandlowski, *Nano Lett.*, 2010, **10**, 156.
8 N. Miyaura, K. Yamada and A. Suzuki, *Tetrahedron Lett.*, 1979, **20**, 3437.
9 R. Perez-Pineiro, S. Dai, R. Alvarez-Puebla, J. Wigginton, B. J. Al-Hourani and H. Fenniri, *Tetrahedron Lett.*, 2009, **50**, 5467.
10 H. A. van Kalkeren, S. H. A. M. Leenders, C. R. A. Hommersom, F. P. J. T. Rutjes and F. L. van Delft, *Chem. – Eur. J.*, 2011, **17**, 11290.
11 Y. Liu, T. C. Stringfellow, D. Ballweg, I. A. Guzei and R. West, *J. Am. Chem. Soc.*, 2001, **124**, 49.
12 B. Q. Xu and N. J. J. Tao, *Science*, 2003, **301**, 1221.
13 L. Venkataraman, J. E. Klare, I. W. Tam, C. Nuckolls, M. S. Hybertsen and M. L. Steigerwald, *Nano Lett.*, 2006, **6**, 458.
14 S. Y. Park, A. C. Whalley, M. Kamenetska, M. L. Steigerwald, M. S. Hybertsen, C. Nuckolls and L. Venkataraman, *J. Am. Chem. Soc.*, 2007, **129**, 15768.
15 M. T. Gonzalez, S. M. Wu, R. Huber, S. J. van der Molen, C. Schonenberger and M. Calame, *Nano Lett.*, 2006, **6**, 2238.
16 M. Kamenetska, M. Koentopp, A. C. Whalley, Y. S. Park, M. L. Steigerwald, C. Nuckolls, M. S. Hybertsen and L. Venkataraman, *Phys. Rev. Lett.*, 2009, **102**, 126803.
17 Low intensity features at low conductance for compounds **1**, **2**, and **5** do not show corresponding plateaus in the 2D histograms (see Fig. S1†). These features may correspond to through-space or sigma-channel conductance.
18 R. S. Klausen, J. R. Widawsky, M. L. Steigerwald, L. Venkataraman and C. Nuckolls, *J. Am. Chem. Soc.*, 2012, **134**, 4541.
19 L. Venkataraman, J. E. Klare, C. Nuckolls, M. Hybertsen and M. Steigerwald, *Nature*, 2006, **442**, 904.
20 D. Vonlanthen, A. Mishchenko, M. Elbind, M. Neuburger, T. Wandlowski and M. Mayor, *Angew. Chem., Int. Ed.*, 2009, **48**, 8886.
21 See the ESI† for details of computational methods. All energies are referenced to vacuum.

22 L. Venkataraman, Y. S. Park, A. C. Whalley, C. Nuckolls, M. S. Hybertsen and M. L. Steigerwald, *Nano Lett.*, 2007, **7**, 502.
23 M. Dell'Angela, G. Kladnik, A. Cossaro, A. Verdini, M. Kamenetska, I. Tamblyn, S. Y. Quek, J. B. Neaton, D. Cvetko, A. Morgante and L. Venkataraman, *Nano Lett.*, 2010, **10**, 2470.
24 J. G. Simmons, *J. Appl. Phys.*, 1963, **34**, 1793.
25 V. B. Engelkes, J. M. Beebe and C. D. Frisbie, *J. Am. Chem. Soc.*, 2004, **126**, 14287.
26 D. J. Mowbray, G. Jones and K. S. Thygsen, *J. Chem. Phys.*, 2008, **128**, 111103.
27 K. Yoshizawa, *Acc. Chem. Res.*, 2012, **45**, 1612.
28 M. Hybertsen, L. Venkataraman, J. E. Klare, A. C. Whalley, M. L. Steigerwald and C. Nuckolls, *J. Phys.: Condens. Matter*, 2008, **20**, 374115.
29 See the ESI† for a discussion of the minor effects of conformation on electronic energy.
30 For a related study, see W. Chen, H. Li, J. R. Widawsky, C. Appayee, L. Venkataraman and R. Breslow, *J. Am. Chem. Soc.*, 2014, **136**, 918.
31 T. A. Su, J. R. Widawsky, H. Li, R. S. Klausen, J. L. Leighton, M. L. Steigerwald, L. Venkataraman and C. Nuckolls, *J. Am. Chem. Soc.*, 2013, **135**, 18331.

